

Articles

Coordination Chemistry of the 2-Pyridyldiphosphine Ligands, $(\text{py})_2\text{P}(\overline{\text{CH}(\text{CH}_2)_3\text{CH}})\text{P}(\text{py})_2$ and $(\text{py})_2\text{P}(\text{CH}_2)_2\text{P}(\text{py})_2$ ($\text{py} = 2\text{-Pyridyl}$), with Platinum(II) and Ruthenium(II). Ruthenium-Catalyzed Hydrogenation of Imines[†]

Nathan D. Jones,[‡] Kenneth S. MacFarlane,[‡] Martin B. Smith,[§] Richard P. Schutte,[‡] Steven J. Rettig,^{†,‡} and Brian R. James^{*,‡}

Department of Chemistry, The University of British Columbia, Vancouver, B.C., V6T 1Z1, Canada, and Department of Chemistry, Loughborough University, Loughborough, Leicestershire, LE11 3TU, UK

Received January 6, 1999

The synthesis and characterization of a range of Pt(II) and Ru(II) complexes containing the new 2-pyridyldiphosphine ligand, $\text{d}(\text{py})\text{pcp} = (\text{py})_2\text{P}(\overline{\text{CH}(\text{CH}_2)_3\text{CH}})\text{P}(\text{py})_2$ (made as a racemate) and the previously reported $\text{d}(\text{py})\text{pe} = (\text{py})_2\text{P}(\text{CH}_2)_2\text{P}(\text{py})_2$ are given ($\text{py} = 2\text{-pyridyl}$). The Pt complexes made were *cis*-PtX₂($\text{d}(\text{py})\text{pcp}$) (X = Cl (**1**), I (**2**)), *cis*-PtX₂($\text{d}(\text{py})\text{pe}$) (X = Cl (**3**), I (**4**)), [Pt($\text{d}(\text{py})\text{pcp}$)₂][PF₆]₂ (**5**), and [Pt($\text{d}(\text{py})\text{pe}$)₂][PF₆]₂ (**6**); these all contain *P,P*-bonded diphosphine ligand, as evidenced by ³¹P NMR data and by crystallographic data in the case of **2** and **3**. The X-ray structure of $\text{d}(\text{py})\text{pe}$ is also reported. The complexes RuX₂(*P,P,N*- $\text{d}(\text{py})\text{pcp}$)(PPh₃) have *cis*-halogens and a *P,P,N*-bonding mode of the pyridyldiphosphine (which incorporates a four-membered *P,N*-chelate ring) with either a *mer*-arrangement (in **7a**, X = Cl) or a *fac*-arrangement of the three P donor atoms (in **7b** (X = Cl), **8** (X = Br), **9** (X = I)); *cis*-RuCl₂(*dppb*)(*P,N*-PPh₂(*py*)) (**12**) (*dppb* = Ph₂P(CH₂)₄PPh₂) is included because it has a donor set corresponding to that in **7b**. Use of the purely *P,P* donor Ph₂P($\overline{\text{CH}(\text{CH}_2)_3\text{CH}}\text{PPh}_2$) (*dppcp*), made as a racemate, affords *trans*-RuCl₂(*dppcp*)₂ (**10**) and *trans*-RuCl₂(*dppcp*)(*dppb*) (**11**). Crystallographic data for **7a**, **7b**, and **12** are reported together with the NMR data for all the Ru complexes. Preliminary results show that the Ru complexes **7b**, **8**, and **9** are effective precursors for catalytic H₂-hydrogenation of aldimines.

Introduction

The chemistry of heterodifunctional ligands incorporating both “soft” (e.g. P) and “hard” (e.g. N or O) donor atoms continues to attract interest.^{1,2} The coordination chemistry of 2-pyridylphosphines in particular has been extensively studied. In addition to a large number of mononuclear complexes,³ several binuclear species⁴ as well as clusters⁵ and oligomers,⁶ the last three classes employing the ligand in a *P,N*-bridging mode, have been characterized. In addition, some homogeneous

catalytic applications, including hydrogenation,¹ hydroformylation,^{1,4a,7} and carbonylation⁸ have been investigated.

A widely used pyridylphosphine is 2-(diphenylphosphino)pyridine, PPh₂(*py*) (type **I**, Chart 1), which as a ligand can adopt three different coordination modes: *P*-monodentate,⁹ *P,N*-chelate,^{3a,c} and *P,N*-bridge.^{4–6} Di- and trisubstituted 2-pyridylphosphines such as PPh(*py*)₂, P(*py*)₃, and XPPh_{3–*n*}(*py*)_{*n*} (X = O, S, AuCl, Au(C₆F₅); *n* = 2, 3) can take on a variety of

[†] Deceased on Oct. 27, 1998. This paper is dedicated to the memory of Steven Rettig.

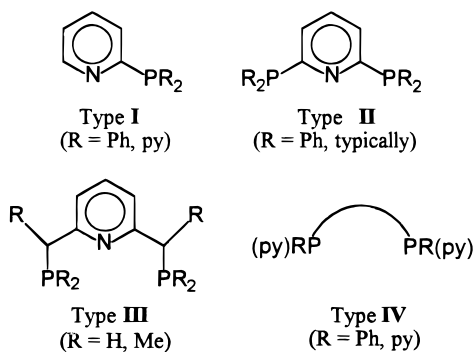
[‡] The University of British Columbia.

[§] Loughborough University.

- (1) For general reviews of *P,N* ligands, see: (a) Zhang, Z.-Z.; Cheng, H. *Coord. Chem. Rev.* **1996**, *147*, 1. (b) Newkome, G. R. *Chem. Rev.* **1993**, *93*, 2067.
- (2) For a general review of *P,O* ligands, see: Bader, A.; Lindner, E. *Coord. Chem. Rev.* **1991**, *108*, 27.
- (3) (a) Nicholson, T.; Hirsch-Kuchma, M.; Shellenbarger-Jones, A.; Davison, A.; Jones, A. G. *Inorg. Chim. Acta* **1998**, *267*, 319. (b) Baird, I. R.; Smith, M. B.; James, B. R. *Inorg. Chim. Acta* **1995**, *235*, 291. (c) Braunstein, P.; Kelly, D. G.; Tiripicchio, A.; Ugozzoli, F. *Bull. Soc. Chim. Fr.* **1995**, *132*, 1083. (d) Arena, C. G.; Bruno, G.; De Munno, G.; Rotondo, E.; Drommi, D.; Faraone, F. *Inorg. Chem.* **1993**, *32*, 1601. (e) Xie, Y.; Lee, C.-L.; Yang, Y.; Rettig, S. J.; James, B. R. *Can. J. Chem.* **1992**, *70*, 751.

- (4) (a) Franciò, G.; Scopelliti, R.; Arena, C. G.; Bruno, G.; Drommi, D.; Faraone, F. *Organometallics* **1998**, *17*, 338. (b) Chan, W.-H.; Zhang, Z.-Z.; Mak, T. C. W.; Che, C.-M. *J. Chem. Soc., Dalton Trans.* **1998**, 803. (c) Kuang, S.-M.; Xue, F.; Zhang, Z.-Z.; Xue, W.-M.; Che, C.-M.; Mak, T. C. W. *J. Chem. Soc., Dalton Trans.* **1997**, 3409. (d) Kuang, S.-M.; Cheng, H.; Sun, L.-J.; Zhang, Z.-Z.; Zhou, Z. Y.; Wu, B.-M.; Mak, T. C. W. *Polyhedron* **1996**, *15*, 3417. (e) Xie, L. Y.; James, B. R. *Inorg. Chim. Acta* **1994**, *217*, 209. (f) De Munno, G.; Bruno, G.; Arena, C. G.; Drommi, D.; Faraone, F. *J. Organomet. Chem.* **1993**, *450*, 263. (g) Reinhard, G.; Hirle, B.; Schubert, U.; Knorr, M.; Braunstein, P.; De Cian, A.; Fischer, J. *Inorg. Chem.* **1993**, *32*, 1656. (h) Zhang, Z.-Z.; Xi, H.-P.; Zhao, W.-J.; Jiang, K.-Y.; Wang, R.-J.; Wang, H.-G.; Wu, Y. *J. Organomet. Chem.* **1993**, *454*, 221. (i) Arena, C. G.; Faraone, F.; Fochi, M.; Lanfranchi, M.; Mealli, C.; Seeber, R.; Tiripicchio, A. *J. Chem. Soc., Dalton Trans.* **1992**, 1847. (j) Rotondo, E.; Bruno, G.; Nicolò, F.; Lo Schiavo, S.; Piraino, P. *Inorg. Chem.* **1991**, *30*, 1195. (k) Maisonnat, A.; Farr, J. P.; Olmstead, M. M.; Hunt, C. T.; Balch, A. L. *Inorg. Chem.* **1982**, *21*, 3961. (l) Alcock, N. W.; Moore, P.; Lampe, P. A. *J. Chem. Soc., Dalton Trans.* **1982**, 207.

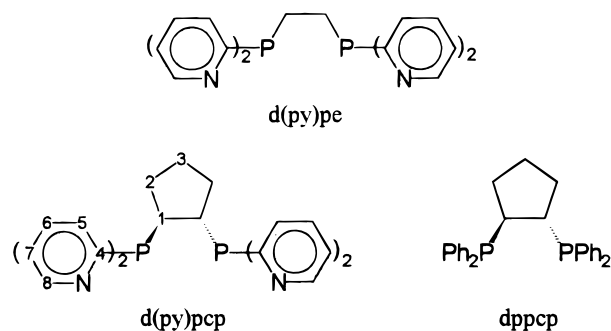
Chart 1



additional coordination modes using a combination of one or more of the group 15/16 donor centers.¹⁰ Recent work within this laboratory has found an unprecedented *P,N,N*-coordination mode for $PPh(py)_2$ and $P(py)_3$.¹¹

In contrast, pyridyldiphosphines have been less studied and, of those documented, two distinct structural classes are apparent. In the first class, two $-PR_2$ moieties (R = Ph, typically) are directly bonded in the 2- and 6-positions of the pyridine ring, affording a *PNP*-ligand system (type II).¹² Ligands of this type readily bridge metal centers and have been used to stabilize both homo- and heterobimetallic complexes. Introduction of a $-CH(R)-$ (R = H, Me) spacer between the $-PPh_2$ groups and the central pyridyl group (type III)¹³ permits extra flexibility within the *PNP*-tridentate ligand and, in the case of R = Me, allows for the synthesis of C_2 -symmetric chiral complexes, some of which have used for the enantioselective hydrogenation of imines.¹⁴ This type of ligand favors bis five-membered chelate ring formation upon coordination to a mononuclear metal

Chart 2



fragment.¹⁵ In the second class, two $-PR(py)$ (R = Ph, py) fragments are linked by an aliphatic carbon spacer of variable length, linear, branched or cyclic (type IV).¹⁶

Our interest in pyridyldiphosphine ligands, especially those of type IV, stems from the idea that protonation of noncoordinated pyridine N atoms on the ligand would be a convenient route to water solubilization of the corresponding metal complexes, with the ultimate objective being the homogeneous catalytic hydration of olefins in aqueous media.^{3b,e} We also believed that catalytic hydrogenation systems might benefit from the inclusion of pyridyldiphosphine ligands in that metal hydride formation via heterolytic H_2 cleavage would be promoted by the presence of an intramolecular base.¹⁷

In this paper we report the synthesis and characterization of a new pyridyldiphosphine containing a cyclopentane ring bridge, racemic- $(py)_2PCH(CH_2)_3CHP(py)_2$ ($d(py)pcp$), isostructural with the tetraphenyl chiral analogue $(Ph)_2PCH(CH_2)_3CHP(Ph)_2$ ($dppcp$) which has been described previously.¹⁸ Both $d(py)pcp$ and the previously reported $(py)_2PC_2H_4P(py)_2$ ($d(py)pe$)^{3b} are potentially hexadentate P_2N_4 ligands, and have been observed to act as such¹⁹ (Chart 2).

Synthetic and characterization details of the coordination chemistry of $d(py)pcp$ and $d(py)pe$ toward a range of Ru(II) and Pt(II) fragments are described, as well as preliminary results for the catalytic hydrogenation of imines using the Ru complexes. The structures of the free ligand $d(py)pe$, the metal complexes $PtCl_2(d(py)pcp)$ ($2 \cdot 0.18CH_2Cl_2$), $PtCl_2(d(py)pe)$ ($3 \cdot CH_2Cl_2$), $RuCl_2(P,P,N-d(py)pcp)(PPh_3)$ ($7a \cdot 2CH_2Cl_2$), $RuCl_2(P,P,N-d(py)pcp)(PPh_3)$ ($7b \cdot 1.5EtOH$), and *cis*- $RuCl_2(dppcp)$ -

- (5) (a) Gobetto, R.; Arena, C. G.; Drommi, D.; Faraone, F. *Inorg. Chim. Acta* **1996**, *248*, 257. (b) Deeming, A. J.; Smith, M. B. *J. Chem. Soc., Chem. Commun.* **1993**, 844 and references therein.
- (6) Braunstein, P.; Knorr, M.; Strampfer, M.; De Cian, A.; Fischer, J. *J. Chem. Soc., Dalton Trans.* **1994**, 117.
- (7) (a) Drommi, D.; Nicolò, F.; Arena, C. G.; Bruno, G.; Faraone, F.; Gobetto, R. *Inorg. Chim. Acta* **1994**, *221*, 109. (b) Gladiali, S.; Pinna, L.; Arena, C. G.; Rotondo, E.; Faraone, F. *J. Mol. Catal.* **1991**, *66*, 183.
- (8) Zhang, Z.-Z.; Xi, H.-P.; Zhao, W.-J.; Jiang, K.-Y.; Wang, R.-J.; Wang, H.-G.; Wu, Y. *J. Organomet. Chem.* **1993**, *454*, 221.
- (9) (a) Xie, Y.; James, B. R. *J. Organomet. Chem.* **1991**, *417*, 277. (b) Newkome, G. R.; Evans, D. W.; Fronczek, F. R. *Inorg. Chem.* **1987**, *26*, 3500. (c) Inoguchi, Y.; Milewski-Mahrla, B.; Neugebauer, D.; Jones, P. G.; Schmidbaur, H. *Chem. Ber.* **1983**, *116*, 1487. (d) Alcock, N. W.; Moore, P.; Lampe, P. A. *J. Chem. Soc., Dalton Trans.* **1982**, 207. (e) Wajda, A.; Pruchnik, F.; Lis, T. *Inorg. Chim. Acta* **1980**, *40*, 207.
- (10) (a) Casares, J. A.; Espinet, P.; Hernando, R.; Iturbe, G.; Villafañe, F.; Ellis, D. D.; Orpen, A. G. *Inorg. Chem.* **1997**, *36*, 44. (b) Casares, J. A.; Espinet, P. *Inorg. Chem.* **1997**, *36*, 5428 and references therein. (c) Schutte, R. P.; Rettig, S. J.; James, B. R. *Can. J. Chem.* **1996**, *74*, 2064. (d) Guillaume, P.; Postel, M. *Inorg. Chim. Acta* **1995**, *233*, 109. (e) Espinet, P.; Gómez-Elipe, P.; Villafañe, F. *J. Organomet. Chem.* **1993**, *450*, 145. (f) Gregorzik, R.; Wirbscher, J.; Vahrenkamp, H. *Chem. Ber.* **1992**, *125*, 1575. (g) Kurtev, K.; Ribola, D.; Jones, R. A.; Cole-Hamilton, D. J.; Wilkinson, G. *J. Chem. Soc., Dalton Trans.* **1980**, 55.
- (11) Schutte, R. P.; Rettig, S. J.; Joshi, A. M.; James, B. R. *Inorg. Chem.* **1997**, *36*, 5809.
- (12) (a) Kuang, S.-M.; Zhang, Z.-Z.; Wang, Q.-G.; Mak, T. C. W. *J. Chem. Soc., Chem. Commun.* **1998**, 581. (b) Zhang, J.-K.; Zhang, Z.-M.; Yu, A.; Zhao, S.-L.; Zhang, W.-D.; Zhang, Z.-Z. *Polyhedron* **1996**, *15*, 2583. (c) McFarlane, H. C. E.; McFarlane, W.; Muir, A. S. *Polyhedron* **1990**, *9*, 1757. (d) Wood, F. E.; Hvoslef, J.; Hope, H.; Balch, A. L. *Inorg. Chem.* **1984**, *23*, 4309 and references therein.
- (13) (a) Jiang, Q.; Van Plew, D.; Murtuza, S.; Zhang, X. *Tetrahedron Lett.* **1996**, *37*, 797. (b) Sablong, R.; Newton, C.; Dierkes, P.; Osborn, J. A. *Tetrahedron Lett.* **1996**, *37*, 4933.
- (14) Sablong, R.; Osborn, J. *Tetrahedron Lett.* **1996**, *37*, 4937.

- (15) (a) Hahn, C.; Sieler, J.; Taube, R. *Polyhedron* **1998**, *17*, 1183 and references therein. (b) Hahn, C.; Vitagliano, A.; Giordano, F.; Taube, R. *Organometallics* **1998**, *17*, 2060. (c) Rahmouni, N.; Osborn, J. A.; De Cian, A.; Fischer, J.; Ezzamarty, A. *Organometallics* **1998**, *17*, 2470, and references therein. (d) Jia, G.; Lee, H. M.; Williams, I. D.; Lau, C. P.; Chen, Y. *Organometallics* **1997**, *16*, 3941.
- (16) (a) Berners-Price, S. J.; Bowen, R. J.; Harvey, P. J.; Healy, P. C.; Koutsantonis, G. A. *J. Chem. Soc., Dalton Trans.* **1998**, 1743. (b) Mirabelli, C. K.; Hill, D. T.; Faucette, L. F.; McCabe, F. L.; Girard, G. R.; Bryan, D. B.; Sutton, B. M.; O'Leary Bartus, J.; Croke, S. T.; Johnson, R. K. *J. Med. Chem.* **1987**, *30*, 2181. (c) Budzelaar, P. H. M.; Frijns, J. H. G.; Orpen, A. G. *Organometallics* **1990**, *9*, 1222.
- (17) James, B. R. In *Comprehensive Organometallic Chemistry*; Wilkinson, G., Stone, F. G. A., Abel, E. W., Eds; Pergamon: Oxford, 1982; Chapter 51.
- (18) (a) Indolese, A. F.; Consiglio, G. *Organometallics* **1994**, *13*, 2230 and references therein. (b) Morandini, F.; Pilloni, G.; Consiglio, G.; Sironi, A.; Moret, M. *Organometallics* **1993**, *12*, 3495 and references therein. (c) Cotton, F. A.; Kang, S.-J. *Inorg. Chim. Acta* **1993**, *209*, 23. (d) Consiglio, G.; Indolese, A. *J. Organomet. Chem.* **1991**, *417*, C36. (e) Alcock, N. W.; Brown, J. M.; Maddox, P. J. *J. Chem. Soc., Chem. Commun.* **1986**, 1532. (f) Allen, D. L.; Gibson, V. C.; Green, M. L. H.; Skinner, J. F.; Bashkin, J.; Grebenik, P. D. *J. Chem. Soc., Chem. Commun.* **1983**, 895.
- (19) Jones, N. D.; Rettig, S. J.; James, B. R. *J. Cluster Sci.* **1998**, *9*, 243.

Table 1. Solution $^{31}\text{P}\{^1\text{H}\}$ NMR Data for Complexes 7–12^a

complex	spin system	P_A	P_M or P_B (ppm)	P_X	$^2J_{AX}$	$^2J_{AM}$ or $^2J_{AB}$ (Hz)	$^2J_{MX}$ or $^2J_{BX}$
<i>mer</i> -RuCl ₂ (d(py)pcp)(PPh ₃), 7a	AMX	38.7 dd	8.0 dd	-7.8 dd	300	24.8	21.0
<i>fac</i> -RuCl ₂ (d(py)pcp)(PPh ₃), 7b	A ₂ X	47.8 d	—	8.8 t	27.7	—	—
<i>fac</i> -RuCl ₂ (d(py)pcp)(PPh ₃), 7b ^b	ABX	48.8 dd	47.5 dd	8.9 dd	26.5	31.1	27.6
<i>fac</i> -RuBr ₂ (d(py)pcp)(PPh ₃), 8	ABX	49.3 dd	49.3 dd	8.3 dd	~27	~31	~27
<i>fac</i> -RuI ₂ (d(py)pcp)(PPh ₃), 9	AMX	48.7 dd	44.7 dd	1.1 dd	24.1	27.6	26.5
<i>trans</i> -RuCl ₂ (dppcp) ₂ , 10 ^c	A ₂ B ₂	22.8 s	23.3 s	—	—	—	—
<i>fac</i> -RuCl ₂ (dppb)(PPh ₂ (py)), 12 ^d	AMX	47.8	36.5	-20.9	26.3	34.6	27.4
		$P_{A(A')}$	$P_{B(B')}$		J values		
<i>trans</i> -RuCl ₂ (dppb)(dppcp), 11 ^e	AA'BB'	16.5	7.1		$^2J_{AB}$ 313.8, $^2J_{A'B'}$ 312.1 $^2J_{AA'}$ 32.0, $^2J_{BB'}$ 34.8 $^2J_{AB'}$ (or $^2J_{A'B}$) -39.6 $^2J_{A'B}$ (or $^2J_{AB'}$) -39.1		

^a Complexes dissolved in CDCl₃ at r.t. unless otherwise indicated; all dd signals are overlapping except for $\delta(P_A)$ and $\delta(P_B)$ for **7a**. ^b In C₆D₆. ^c Mixture of two diastereomers. ^d Taken from ref 11, in which the complex is described as *cis*-RuCl₂(dppb)(PPh₂(py)) for the *cis* disposition of the chloro ligands. ^e A, A' refer to dppb, and B, B' to dppcp; data obtained using the program "NMR" Version 1.0 by Calleo Scientific Software; $^2J_{AB}$ and $^2J_{A'B'}$ are due to the *trans* disposed P atoms, and other 2J values arise from mutually *cis* P atoms.

(PPh₂(py))·2.5 CDCl₃ (**12**) (dppb = Ph₂P(CH₂)₄PPh₂) have been determined by single-crystal X-ray diffraction.

Experimental Section

General Methods and Materials. Unless otherwise stated, manipulations were carried out under Ar using standard Schlenk techniques. Reagent grade solvents (Fisher Scientific) were distilled from CaH₂ (CH₂Cl₂), Na (Et₂O, C₆H₆, and hexanes), Mg/I₂ (MeOH and EtOH), or anhydrous K₂CO₃ (acetone) under N₂.

The complexes RuCl₂(PPh₃)₃,²⁰ RuCl₂(dppb)(PPh₃),²¹ *cis*-RuCl₂(dppb)(PPh₂(py)) (**12**),¹¹ and PtCl₂(cod)²² were prepared according to published procedures. PtI₂(cod) was prepared by metathesis of PtCl₂(cod) using a 5-fold excess of NaI (per chloride) in acetone. PPh₃ and dppb were used as received from Aldrich. Ph₂P(py) was synthesized and characterized as described previously,^{9c} the synthesis being adapted from a literature procedure.²³ The ligand d(py)pe,^{3b} *trans*-1,2-bis(dichlorophosphino)cyclopentane ((Cl₂P)₂C₅H₈) and racemic *trans*-1,2-bis(diphenylphosphino)cyclopentane (dppcp) were prepared as described in the literature.^{18f}

The following reagents were used as supplied: ⁿBuLi (1.6 M in hexanes, Aldrich), NaBr (Anachemia Chemicals Ltd.), NaI (MCB), and NH₄PF₆ (Ozark-Mahoning), NaOH (Fisher), concentrated HCl (Fisher), H₂SO₄ (Fisher), and 2-bromopyridine (Aldrich). The deuterated solvents (CDCl₃, C₆D₆, CD₃OD, CD₂Cl₂, and D₂O) were obtained from Cambridge Isotope Laboratories (CIL); CDCl₃ and C₆D₆ were dried over activated molecular sieves (Fisher: type 4 Å, 4–8 mesh), deoxygenated, and stored under Ar.

Solution NMR spectra were recorded on Varian XL300 (121.42 MHz for $^{31}\text{P}\{^1\text{H}\}$, 75.429 MHz for $^{13}\text{C}\{^1\text{H}\}$), Bruker AC200 (81.015 MHz for $^{31}\text{P}\{^1\text{H}\}$, 50.323 MHz for $^{13}\text{C}\{^1\text{H}\}$), or Bruker AM400 spectrometers; residual solvent proton (¹H) or external P(OMe)₃ ($^{31}\text{P}\{^1\text{H}\}$: δ 141.00 vs external 85% aq. H₃PO₄) or solvent carbon (¹³C) was used as the reference (s = singlet; d = doublet; t = triplet; qn = quintet; spt = septet; m = multiplet; br = broad; p = pseudo). The solution $^{31}\text{P}\{^1\text{H}\}$ NMR data for the Ru complexes are given in the Results and Discussion section (Table 1). The ¹H NMR data are presented in this section for purposes of characterization; peak assignments for d(py)pcp and its dioxide, according to the numbering scheme shown in Chart 2, were made on the basis of COSY experiments, chemical shift values, and coupling constants. All J values are given in Hz. Peaks in the ¹³C-

¹H} NMR spectra of the ligand d(py)pcp and its dioxide have been assigned where possible on the basis of ¹³C-¹H HETCOR and APT experiments. These peaks generally appear as multiplets due to coupling to ³¹P, and, although the coupling constants have not been determined, the number of lines observed in each case is given in parentheses following the peak frequency.

The UV-vis spectra were recorded on a Hewlett-Packard 8452A diode array spectrophotometer and are given as λ_{max} (nm), [ϵ (M⁻¹ cm⁻¹)], sh = shoulder. IR spectra (Nujol mulls, KBr plates) were recorded (cm⁻¹) on an ATI Mattson Genesis FTIR spectrometer (s = strong). Elemental analyses were performed by Mr. P. Borda of the UBC Chemistry department.

The procedure used to screen the activity of the Ru complexes for H₂ hydrogenation of imines to amines, at 1000 psi H₂, including the sources of imines and amines, has been described elsewhere.²⁴

Racemic d(py)pcp. To Et₂O (100 mL) cooled to -77 °C in a dry ice/acetone bath, ⁿBuLi (100 mL, 160 mmol) was added by cannula, and the mixture allowed to cool for 5 min. To this solution was added 2-bromopyridine (16 mL, 160 mmol) which caused an immediate color change from pale yellow to brown-red. The cooled mixture on being stirred for 4 h became deep red. *trans*-1,2-(Cl₂P)₂C₅H₈ (7 mL, 40 mmol) in Et₂O (30 mL) was then added dropwise over 15 min, and stirring was continued for 2 h at -77 °C. This resulted in the formation of a brown suspension. The mixture was then allowed to warm to room temperature (r.t.), whereupon the slurry was extracted with H₂SO₄ (2 × 100 mL, 2 M) and the red aqueous layer was removed by cannula from the yellow organic layer. The extract was neutralized by the dropwise addition of saturated NaOH (~35 mL) which resulted in the formation of an "oily mass". This mixture was filtered to yield a dark orange grease which was re-suspended in acetone (60 mL) to give a fine, white powder and red-brown filtrate. The solid was collected, washed with acetone (3 × 2 mL) and then thoroughly with H₂O (~150 mL). Reprecipitation from acetone/hexanes yielded a cream-colored solid which was collected and then dried under vacuum at 100 °C for 72 h. Yield: 6.28 g (35%). Anal. Calcd for C₂₅H₂₄N₄P₂: C, 67.87; H, 5.47; N, 12.66. Found: C, 67.86; H, 5.45; N 12.58. ¹H NMR (C₆D₆, 400 MHz, 20 °C): δ 1.74 (qn, 2H³, $^3J_{\text{HH}} = 5.3$), 1.97 (m, 2H²), 2.38 (m, 2H²), 3.90 (ddd, 2H¹, $^2J_{\text{HP}} = 11.47$, $^3J_{\text{HH(anti)}} = 7.78$, $^3J_{\text{HH(gauche)}} = 3.21$), 6.47 (dd, 2H⁷, $^3J_{\text{HH}} = 4.8$, $^3J_{\text{HH}} = 7.6$), 6.51 (dd, 2H⁷, $^3J_{\text{HH}} = 4.8$, $^3J_{\text{HH}} = 7.6$), 6.87 (m, 4H⁶), 7.32 (m, 2H⁵), 7.46 (m, 2H⁵); this pattern could be simulated with unassigned coupling constants of 7.7, 1.9, and 1.8 Hz), 8.38 (pd, 2H⁸, $^3J_{\text{HH}} = 10.1$), 8.49 (pd, 2H⁸, $^3J_{\text{HH}} = 10.1$). ¹³C{¹H} NMR (50.323 MHz, CDCl₃, 20 °C): δ 25.1 (3, C³), 30.2 (3, C²), 39.1 (4, C¹), 122.5 (2), 129.3 (8), 135.2 (4, C⁶), 149.8 (6, C⁸) 162.9 (1, C⁴). ³¹P{¹H} NMR (121.4 MHz, CDCl₃, 20 °C): δ -2.2 (s). The diphosphine was made as a mixture of *R,R*- and *S,S*-

(20) Hallman, P. S.; Stephenson, T. A.; Wilkinson, G. *Inorg. Synth.* **1970**, *12*, 237.

(21) (a) Joshi, A. M.; Thorburn, I. S.; Rettig, S. J.; James, B. R. *Inorg. Chim. Acta* **1992**, *198*, 283. (b) Jung, C. W.; Garrou, P. E.; Hoffman, P. R.; Caulton, K. G. *Inorg. Chem.* **1984**, *23*, 726.

(22) McDermott, J. X.; White, J. F.; Whitesides, G. M.; *J. Am. Chem. Soc.* **1976**, *98*, 6521.

(23) Kurtev, K.; Ribola, D.; Jones, R. A.; Cole-Hamilton, D. J.; Wilkinson, G. *J. Chem. Soc., Dalton Trans.* **1980**, 55.

(24) (a) Fogg, D. E.; James, B. R.; Kilner, M. *Inorg. Chim. Acta* **1994**, *222*, 85. (b) Fogg, D. E.; James, B. R. *Chem. Ind. (Dekker)* **1995**, 62, 435.

enantiomers, the chirality designators referring to the C¹ atoms of the cyclopentane backbone.

Racemic d(py)pcp(O)₂. To a 0.2 M HCl solution (15 mL) containing d(py)pcp (160 mg, 0.36 mmol) in a flask open to the atmosphere was added dropwise a 30% H₂O₂ solution (2 mL). The colorless solution was stirred for 1 h, cooled on ice, and then made basic using a saturated KOH solution. The aqueous phase was extracted with CH₂Cl₂ (3 × 25 mL) and the combined organic fractions dried over MgSO₄. This mixture was filtered and the filtrate reduced to ~2 mL under reduced pressure. Et₂O (30 mL) was then added to afford the product as a white precipitate, which was collected, washed with Et₂O (3 × 3 mL), and dried in vacuo. Yield: 91 mg (53%). Anal. Calcd for C₂₅H₂₄N₄O₂P₂: C, 63.29; H, 5.10; N, 11.81. Found: C, 63.11; H, 5.13; N 11.82. ¹H NMR (300 MHz, D₂O, 20 °C): δ 1.55 (m, 2H, CH₂), 1.70 (br m, 2H, CH₂), 1.92 (br m, 2H, CH₂), 3.64 (br m, 2H, CH), 7.15 (m, 2H, py), 7.32 (m, 2H, py), 7.62 (br m, 4H, py), 7.71 (br m, 4H, py), 7.90 (pd, 2H, py), 8.45 (pd, 2H, py). ¹³C{¹H} NMR (CDCl₃, 75.429 MHz, 20 °C): δ 26.2 (1, C³), 28.8 (1, C²), 35.0 (2, C²), 124.7 (2), 128.2 (5), 135.5 (2, C⁶), 150.0 (5, C⁸), 168.2 (1, C⁴). ³¹P{¹H} NMR (121.4 MHz, 20 °C): δ 35.8 (s) [CDCl₃]; 38.7 (s) [D₂O]. IR: ν_{PO} = 1194 cm⁻¹.

cis-PtCl₂(d(py)pcp), 1. A CH₂Cl₂ (10 mL) solution of d(py)pcp (104 mg, 0.24 mmol) was added dropwise via cannula over 5 min to a CH₂-Cl₂ (5 mL) solution of PtCl₂(cod) (93 mg, 0.25 mmol). The resulting colorless solution was stirred for 1 h, and the volume was then reduced to ~2 mL. The product was afforded as a fine white precipitate by the addition of Et₂O (30 mL), isolated by filtration, and washed with Et₂O (3 × 5 mL). Reprecipitation from CH₂Cl₂ and drying in vacuo at 100 °C yielded pure product. Yield: 144 mg (86%). Anal. Calcd for C₂₅H₂₄N₄Cl₂P₂Pt: C, 42.38; H, 3.47; N, 7.91. Found: C, 42.62; H, 3.40; N, 7.64. ¹H NMR (200 MHz, CDCl₃, 20 °C): δ 1.6 (m, 2H, CH₂), 2.1 (m, 4H, CH₂), 3.6 (pt, 2H, CH), 7.3–8.8 (m, 16H, py). ³¹P-{¹H} NMR (81.015 MHz, CDCl₃, 20 °C): δ 17.86 (s, ¹J_{Pt} = 3493).

cis-PtI₂(d(py)pcp), 2. Preparation of **2** in the same manner as that outlined for **1** yielded, in addition, a small quantity of [Pt(d(py)pcp)₂]-I₂, as determined by ³¹P{¹H} NMR spectroscopy (see **5** below). This contaminant was removed by washing the product with dilute HCl (~50 mL). Thus, reaction of PtI₂(cod) (100 mg, 0.18 mmol) and d(py)pcp (79 mg, 0.18 mmol) yielded 129 mg (80%) of a yellow powder. Anal. Calcd for **2**, C₂₅H₂₄N₄I₂P₂Pt: C, 33.69; H, 2.71; N, 6.29. Found: C, 34.08; H, 2.72; N, 6.00. ¹H NMR (300 MHz, CDCl₃, 20 °C): δ 1.55 (m, 2H, CH₂), 1.75 (m, 2H, CH₂), 2.10 (m, 2H, CH₂), 3.65 (2H, m, CH), 7.3–8.8 (m, 16H, py). ³¹P{¹H} NMR (121.4 MHz, CDCl₃, 20 °C): δ 12.57 (s, ¹J_{Pt} = 3294). Crystals of **2**·0.18 CH₂Cl₂ were isolated after 72 h from a CH₂Cl₂ solution of **2** onto which Et₂O had been layered.

cis-PtCl₂(d(py)pe), 3. Compound **3** was prepared in the same manner as **1**, except that the product was washed with MeOH instead of Et₂O. Reaction of PtCl₂(cod) (225 mg, 0.60 mmol) and d(py)pe (243 mg, 0.60 mmol) yielded 300 mg (70%) of a white powder. Anal. Calcd for C₂₂H₂₀N₄Cl₂P₂Pt: C, 39.54; H, 3.02; N, 8.38. Found: C, 39.74; H, 3.00; N, 8.10. ¹H NMR (300 MHz, CDCl₃, 20 °C): δ 2.9 (m, 4H, CH₂), 7.4–8.7 (m, 16H, pyridyl). ³¹P{¹H} NMR (121.4 MHz, CDCl₃, 20 °C): δ 47.08 (s, ¹J_{Pt} = 3481). Colorless crystals of **3**·CH₂Cl₂, suitable for study by X-ray diffraction, were isolated after 24 h from a CH₂Cl₂ solution of **3**, which had been layered with Et₂O.

cis-PtI₂(d(py)pe), 4. Compound **4** was prepared in the same manner as **1**. Reaction of PtI₂(cod) (71 mg, 0.13 mmol) and d(py)pe (51 mg, 0.13 mmol) yielded 50 mg (46%) of a yellow powder. Anal. Calcd for C₂₂H₂₀N₄I₂P₂Pt: C, 31.04; H, 2.37; N, 6.58. Found: C, 31.17; H, 2.44; N, 6.35. ¹H NMR (300 MHz, CD₂Cl₂, 20 °C) δ 2.73 (m, 4H, CH₂), 7.25–8.85 (m, 16H, py). ³¹P{¹H} NMR (121.4 MHz, CDCl₃, 20 °C) δ 49.84 (s, ¹J_{Pt} = 3397).

Preparations of the compounds [Pt(L)₂]₂ (L = d(py)pe, d(py)pcp; X = Cl, I) either by reaction of 2 equiv of the ligand with PtX₂(cod) in CH₂Cl₂ or, in the case of the iodide salts, by metathesis of [Pt(L)₂]-Cl₂ with NaI in acetone, were successful as determined by ¹H and ³¹P-{¹H} NMR spectroscopies. However, satisfactory elemental analyses were not obtained for these complexes.

[Pt(d(py)pcp)₂][PF₆]₂·H₂O, 5·H₂O. To a Schlenk tube charged with PtCl₂(cod) (14.1 mg, 38 μmol), d(py)pcp (34.0 mg, 77 μmol) and NH₄-PF₆ (12.7 mg, 78 μmol) were added CH₂Cl₂ (3 mL) and acetone (4

mL). The resulting cloudy mixture was stirred at r.t. for 75 min and then filtered through Celite 545. The volume of the colorless filtrate was reduced to ~2 mL under vacuum, and the product, afforded as a white precipitate by the addition of Et₂O (20 mL), was isolated by filtration and dried overnight in vacuo. Yield: 39 mg (73%). Anal. Calcd for C₅₀H₅₀N₈F₁₂OP₆Pt: C, 43.27; H, 3.78; N, 8.07. Found: C, 43.07; H, 3.60; N, 8.00. ¹H NMR (400 MHz, CDCl₃, 20 °C): δ 1.27 (br m, 4H, CH₂), 1.72 (m, 4H, CH₂), 2.13 (m, 4H, CH₂), 3.45 (m, 4H, CH), 7.15–8.75 (m, 32H, py). ³¹P{¹H} NMR (81.015 MHz, CDCl₃, 20 °C): δ 18.35 (s, ¹J_{Pt} ≈ 2400), 18.44 (s, ¹J_{Pt} = 2404), -144 (spt, ¹J_{PF} = 712, PF₆⁻).

[Pt(d(py)pe)₂][PF₆]₂, 6. An impure sample of [Pt(d(py)pe)₂]₂Cl₂ (50 mg, ~47 μmol, see above) and NH₄PF₆ (16 mg, 98 μmol) were dissolved in acetone (20 mL), and the resulting cloudy solution was stirred for 30 min; the mixture was filtered through Celite 545 which was subsequently washed with acetone (3 × 5 mL) and the combined filtrate reduced to ~2 mL. The product was afforded as a white precipitate by the addition of Et₂O (30 mL), isolated by filtration, washed with Et₂O (3 × 5 mL), and dried in vacuo. Yield: 42 mg (77%). Anal. Calcd for C₅₀H₄₈N₈F₁₂P₆Pt: C, 40.98; H, 3.13; N, 8.69. Found: C, 40.82; H, 2.98; N, 8.51. ¹H NMR (300 MHz, CD₃OD, 20 °C): δ 1.30 (m, 8H, CH₂), 5.7–7.1 (m, 32H, py). ³¹P{¹H} NMR (81.015 MHz, CD₃OD, 20 °C): δ 54.42 (s, ¹J_{Pt} = 2477), -144 (spt, ¹J_{PF} = 712, PF₆⁻).

RuCl₂(P,P,N-d(py)pcp)(PPh₃)·H₂O, 7a·H₂O (“mer-Isomer”) and 7b·H₂O (“fac-Isomer”). A 1 equiv amount of d(py)pcp (230 mg, 0.52 mmol) was added to a CH₂Cl₂ (20 mL) solution of RuCl₂(PPh₃)₃ (500 mg, 0.52 mmol) and the resulting dark brown mixture stirred at r.t. After 20 min, the dark orange solution was reduced to dryness and the residue taken up in a 1:1 mixture of CH₂Cl₂ and C₆H₆ (10 mL). Hexanes (10 mL) were added to precipitate the yellow-orange product, which was collected, washed with hexanes (3 × 5 mL), and dried under vacuum at 100 °C. The solid was shown by ³¹P{¹H} NMR spectroscopy (see Table 1) to be complex **7b**·H₂O. Yield: 0.31 g (67%). Anal. Calcd for C₄₃H₄₁N₄Cl₂OP₃Ru: C, 57.72; H, 4.62; N, 6.26. Found: C, 57.97; H, 4.54; N, 6.13. ¹H NMR of **7b** (300 MHz, CDCl₃, 20 °C): δ 0.24 (br m, 1H, CH), 1.36 (m, 2H, CH₂), 1.56 (s, H₂O), 1.95 (m, 2H, CH₂), 2.42 (br m, 1H, CH₂), 2.68 (br m, 1H, CH₂), 3.62 (br m, 1H, CH), 6.8–8.6 (m, 31H, py and Ph). UV–vis (CH₂Cl₂): 344 [3090], 420 [1670]. ³¹P{¹H} NMR spectroscopy showed that **7a** constituted a small fraction of the dissolved Ru in the CH₂Cl₂/C₆H₆/hexanes filtrate; by slow evaporation of this mixture a bright orange crystal of **7a**·2CH₂-Cl₂ was isolated. Subsequently, an X-ray diffraction quality orange crystal of the major isomer (**7b**) was isolated as **7b**·1.5EtOH from a CH₂Cl₂ solution of the complex which had been layered with EtOH. Assignment of the ¹H NMR spectrum of **7a** was impossible due to overlapping resonances of **7b**.

A mixture of **7a** and **7b** hydrates can also be prepared by stirring the two reactants in C₆D₆ at r.t. for 3 h.

RuBr₂(P,P,N-d(py)pcp)(PPh₃)·H₂O, 8. Excess NaBr (140 mg, 1.4 mmol) was added to an acetone solution (10 mL) of **7b**·H₂O (52 mg, 0.058 mmol) and the resulting cloudy yellow-orange suspension stirred for 24 h at r.t. The mixture was pumped to dryness and the orange-brown residue dissolved in CH₂Cl₂; this was then filtered through Celite 545, and the solution reduced in volume to ~3 mL. Et₂O (20 mL) and hexanes (10 mL) were added to precipitate the orange product which was collected, washed with hexanes (2 × 3 mL), and dried under vacuum. Yield: 39 mg (67%). Anal. Calcd for C₄₃H₄₁N₄Br₂OP₃Ru: C, 52.51; H, 4.20; N, 5.70. Found: C, 52.64; H, 4.14; N, 5.54. ¹H NMR (300 MHz, CDCl₃, 20 °C): δ 0.10 (m, 1H, CH), 1.40 (m, 2H, CH₂), 1.56 (s, H₂O), 1.90 (m, 2H, CH₂), 2.30 (br m, 1H, CH₂), 2.64 (br m, 1H, CH₂), 3.65 (br m, 1H, CH), 6.7–8.7 (m, 31H, py and Ph). UV–vis (CH₂Cl₂): 350 [2320], 430 [1370].

RuI₂(P,P,N-d(py)pcp)(PPh₃)·H₂O, 9. Excess NaI (140 mg, 0.93 mmol) was added to an acetone solution (10 mL) of **7b**·H₂O (41 mg, 0.046 mmol) and the resulting cloudy orange suspension stirred for 18 h at r.t. The mixture was pumped to dryness and the orange-brown residue dissolved in CH₂Cl₂ (10 mL); this was filtered through Celite 545, and the solution reduced in volume to ~3 mL. Et₂O (20 mL) was added to precipitate the orange product which was collected, washed with Et₂O (5 mL), and dried under vacuum. Yield: 29 mg (67%). Anal.

Table 2. Crystallographic Data

	d(py)pe	2·0.18CH ₂ Cl ₂	3·CH ₂ Cl ₂	7a·2CH ₂ Cl ₂	7b·1.5EtOH	12
formula	C ₂₂ H ₂₀ N ₄ P ₂	C _{25.18} H _{24.36} N ₄ Cl _{0.36} I ₂ P ₂ Pt	C ₂₃ H ₂₂ N ₄ Cl ₄ P ₂ Pt	C ₄₅ H ₄₃ N ₄ Cl ₆ P ₃ Ru	C ₄₆ H ₄₈ N ₄ Cl ₂ O _{1.5} P ₃ Ru	C _{47.5} H ₄₂ NCl _{9.5} D _{2.5} P ₃ Ru
fw	402.37	906.63	753.30	1046.51	945.76	1162.68
crystal system	monoclinic	monoclinic	monoclinic	triclinic	triclinic	triclinic
space group	<i>P</i> 2 ₁ / <i>n</i> (No. 14)	<i>P</i> 2 ₁ / <i>c</i> (No. 14)	<i>P</i> 2 ₁ / <i>n</i> (No. 14)	<i>P</i> 1 (No. 2)	<i>P</i> 1 (No. 2)	<i>P</i> 1 (No. 2)
<i>a</i> , Å	11.615(1)	17.359(1)	8.452(2)	10.413(1)	12.187(1)	11.905(2)
<i>b</i> , Å	5.800(3)	19.207(1)	16.351(4)	12.457(1)	17.432(1)	19.210(2)
<i>c</i> , Å	15.538(2)	19.287(1)	19.794(2)	19.298(1)	21.024(1)	11.569(1)
α , deg	90	90	90	78.896(1)	97.882(1)	98.795(2)
β , deg	106.465(7)	110.464(1)	97.49(1)	88.024(1)	91.845(1)	104.042(1)
γ , deg	90	90	90	65.951(1)	95.422(1)	78.148(4)
<i>V</i> , Å ³	1003.8(5)	6024.6(6)	2712.1(8)	2256.53(6)	4399.7(4)	2496.9(5)
<i>Z</i>	2	8	4	2	4	2
<i>D</i> _{calc} , g/cm ³	1.331	1.999	1.845	1.549	1.428	1.546
<i>T</i> , °C	21	-93	21	-100	-100	-93
λ , Å	0.710 69	0.710 69	0.710 69	0.710 69	0.710 69	0.710 69
μ , cm ⁻¹	2.25	68.48	56.85	8.52	6.28	9.53
<i>R</i>	0.049 ^a	0.048 ^a	0.031 ^a	0.0456 ^b	0.0541 ^b	0.058 ^b
<i>R</i> _w	0.048 ^a	0.050 ^a	0.029 ^a	0.0913 ^b	0.1115 ^b	0.098 ^b

^a $R = \sum(|F_o| - |F_c|) / \sum|F_o|$, $R_w = [\sum w(|F_o| - |F_c|)^2 / \sum w|F_o|^2]^{1/2}$ (based on reflections with $I > 3\sigma(I)$). ^b $R = \sum(|F_o| - |F_c|) / \sum|F_c|$ (based on reflections with $I > n\sigma(I)$, $n = 2$ for **7a** and **7b**, $n = 3$ for **12**), $R_w = [\sum w(|F_o|^2 - |F_c|^2)^2 / \sum w|F_o|^2]^{1/2}$ (based on all data).

Calcd for C₄₃H₄₁N₄I₂OP₃Ru: C, 47.93; H, 3.83; N, 5.20. Found: C, 47.97; H, 3.82; N, 5.04. ¹H NMR (200 MHz, CDCl₃, 20 °C): δ 0.10 (m, 1H, CH), 1.30 (m, 2H, CH₂), 1.56 (s, H₂O), 1.85 (m, 2H, CH₂), 2.15 (br m, 1H, CH₂), 2.62 (br m, 1H, CH₂), 3.64 (br m, 1H, CH), 6.7–8.9 (m, 31H, py and Ph). UV–vis (CH₂Cl₂): 360 [4000], 452 [2160].

trans-RuCl₂(dppcp)₂, 10. Method 1. RuCl₂(PPh₃)₃ (260 mg, 0.27 mmol) and dppcp (120 mg, 0.27 mmol) were dissolved in CH₂Cl₂ (10 mL) and the solution stirred at r.t. After 2 h, the brown suspension was concentrated ~5 mL and EtOH (10 mL) was added to precipitate a beige solid which was collected, washed with EtOH (2 × 5 mL), and dried under vacuum. Yield: 50 mg (36% based on phosphine). The initial aim of this procedure was to prepare the complex RuCl₂(dppcp)(PPh₃), and thus only 1 equiv of the phosphine was used. The excess RuCl₂(PPh₃)₃ remained in solution (and was separated from the product by filtration); the yield would certainly have been improved by using two equivs of phosphine.

Method 2. **10** could be prepared more conveniently by refluxing an EtOH (25 mL) solution of RuCl₃·xH₂O (250 mg, 1.0 mmol, 41.50% Ru) and dppcp (930 mg, 2.1 mmol) for 5 h. The resulting light-colored precipitate was collected, washed with EtOH (10 mL), and dried under vacuum. Yield: 710 mg (67%). Anal. Calcd for C₅₈H₅₆Cl₂P₄Ru: C, 66.41; H, 5.38; Cl, 6.76. Found: C, 66.16; H, 5.36; Cl, 7.03. ¹H NMR (300 MHz, CDCl₃, 20 °C): δ 0.55 (br m, 2H, CH₂), 1.30 (br m, 4H, CH₂), 1.62 (br m, 4H, CH₂), 1.83 (br m, 2H, CH₂), 3.55 (br m, 4H, CH), 6.80–7.90 (m, 40H, Ph).

trans-RuCl₂(dppb)(dppcp), 11. To a C₆H₆ (30 mL) solution of RuCl₂(dppb)(PPh₃) (220 mg, 0.25 mmol) was added dppcp (120 mg, 0.27 mmol), and the resulting solution was stirred at 20 °C for 1 h. The orange-brown solution was reduced in volume to ~5 mL, and hexanes (35 mL) were then added to precipitate a beige solid, which was collected, washed with hexanes (3 × 5 mL), and dried under vacuum. Yield: 190 mg (73%). Anal. Calcd for C₅₇H₅₆Cl₂P₄Ru: C, 66.02; H, 5.44; Cl, 6.84. Found: C, 66.23; H, 5.60; Cl, 7.00. ¹H NMR (300 MHz, CHCl₃, 20 °C): δ 0.65 (br m, 2H, CH₂ of dppcp), 1.32 (br m, 4H, CH₂ of dppb), 2.12 (br m, 2H, CH₂ of dppcp), 2.19 (br m, 2H, CH₂ of dppcp), 2.25 (br m, 2H, CH₂ of dppb), 2.69 (br m, 2H, CH₂ of dppb), 3.45 (br m, 2H, CH of dppcp), 6.42–8.02 (m, 40H, Ph).

RuCl₂(dppb)(*P,N*-PPh₂(py))·2.5CDCl₃, 12. Orange crystals of **12** were isolated, after several months at r.t., from an NMR tube containing a CDCl₃ solution of the complex which had been prepared according to ref 11. The structure is included here because of its similarity to those of **7b**, **8**, and **9**, with a *fac*-arrangement of P atoms.

X-ray Crystallographic Analyses. The solvate molecules associated with each structure are omitted in this section for ease of reading; e.g. 2·0.18 CH₂Cl₂ is written simply as **2**.

Crystallographic data appear in Table 2. The final unit-cell parameters were obtained by least-squares based on 25 reflections with

$2\theta = 15.1$ – 27.4° for d(py)pe, 37963 reflections with $2\theta = 4.0$ – 60.4° for **2**, 25 reflections with $2\theta = 20.9$ – 30.6° for **3**, 6925 reflections with $2\theta = 2.16$ – 50.06° for **7a**, 5711 reflections with $2\theta = 1.96$ – 50.12° for **7b**, and 17 370 reflections with $2\theta = 4.0$ – 60.1° for **12**. The intensities of three standard reflections, measured every 200 reflections throughout the data collections for d(py)pe and **3**, decreased linearly by 3.2% and 16.3%, respectively. The data were processed,^{25,26} corrected for Lorentz and polarization effects, decay (for d(py)pe, **2** and **3**), and absorption (empirical, based on azimuthal scans for d(py)pe and **3**, semiempirical for **7a**, SADABS for **7b**, and fourth-order spherical harmonics for **12**).

The structure analysis of **12** was initiated in the centrosymmetric space group *P* on the basis of the *E* statistics, this choice being confirmed by subsequent calculations. The structures of **2**, **3**, and **12** were determined by the Patterson method and those of d(py)pe, **7a**, and **7b** were determined by direct methods. The d(py)pe molecule lies on a crystallographic center of symmetry. There are two independent molecules, and a partial CH₂Cl₂ molecule, in the asymmetric unit of **2**. The asymmetric unit of **3** contains one metal complex and one CH₂Cl₂ molecule, while that of **7a** contains one metal complex and two CH₂Cl₂ molecules, and that of **12** consists of one metal complex and 2.5 molecules of CDCl₃. One of the CDCl₃ molecules in **12** is (1:1) disordered about an inversion center, one is ordered in a general position, and the third is (1:1) 2-fold disordered with respect to rotation about the C–D bond. The asymmetric unit of **7b** consists of two Ru complexes and three EtOH molecules.

Some half-occupancy non-hydrogen atoms in **12** (Cl(9), Cl(12), and C(47)) were refined with isotropic thermal parameters because the anisotropic thermal parameters were nonpositive-definite. All remaining non-hydrogen atoms were refined with anisotropic thermal parameters. The hydrogen atom positions of d(py)pe, **2**, **3**, and **12** were fixed in calculated positions (C–H = 0.98 Å, *B*_H = 1.2*B*_{bonded atom}). The hydrogen atoms for **7a** and **7b** were placed in ideal positions and refined as riding atoms with individual (or group if appropriate) isotropic displacement parameters. Corrections for secondary extinction (Zachariasen type, isotropic) were applied where necessary, the final values of the extinction coefficients being 6.6(3) × 10⁻⁶ for d(py)pe and 6.2(15) × 10⁻⁷ for **3**. Neutral atom scattering factors for all atoms and anomalous dispersion corrections for the non-hydrogen atoms were taken from the *International Tables for Crystallography*.²⁷

(25) *teXsan: Crystal Structure Analysis Package*; Molecular Structure Corporation: The Woodlands, TX, 1997.

(26) *d*trek: Area Detector Software*; Molecular Structure Corporation: The Woodlands, TX, 1997.

(27) (a) *International Tables for X-ray Crystallography*; Kynoch Press: Birmingham, England, 1974; Vol. IV, pp 99–102. (b) *International Tables for Crystallography*; Kluwer Academic Publishers: Boston, 1992; Vol. C, pp 200–206.

Selected bond lengths and bond angles for d(py)pe and the complexes **2**, **3**, **7a**, **7b**, and **12** appear in Tables 3–8, respectively. A complete table of crystallographic data, atomic coordinates and equivalent isotropic thermal parameters, complete tables of bond lengths and bond angles, anisotropic thermal parameters, torsion angles, and intermolecular contacts for the six structures are included as Supporting Information.

Results and Discussion

Syntheses. rac-d(py)pcp and its Dioxide. The racemic d(py)-pcp compound was made via treatment of *trans*-1,2-Cl₂P-(CH(CH₂)₃CH)PCl₂^{18f} with 2-lithiopyridine which itself was formed in situ from 2-bromopyridine.^{3b} The dioxide (py)₂P(O)-(CH(CH₂)₃CH)P(O)(py)₂ (d(py)pcp(O)₂) was synthesized (as a racemate) to establish, by ³¹P NMR spectroscopy, the absence of this compound as a possible impurity in the complexes here under study (particularly those of Ru).

Platinum Complexes. A scheme for the numbering of platinum complexes with the general empirical formula Pt-(P-P)_nX₂ (*n* = 1, 2; P-P = d(py)pe, d(py)pcp; X = Cl, I, PF₆) is given below.

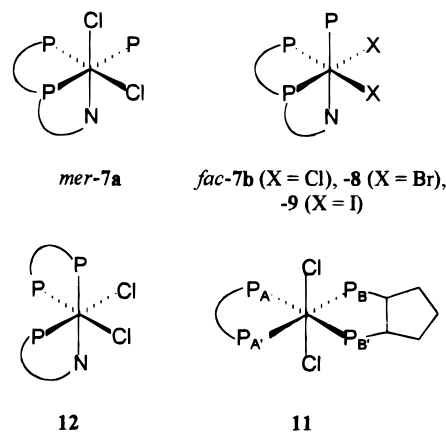
	P-P = d(py)pcp	P-P = d(py)pe
<i>n</i> = 1, X = Cl	1	3
<i>n</i> = 1, X = I	2	4
<i>n</i> = 2, X = PF ₆	5	6

Addition of 1 equiv of d(py)pe or d(py)pcp to PtX₂(cod) (X = Cl, I) results in the rapid formation of the *P,P*-bonded complexes PtX₂(P-P), although in the case of X = I, a small amount of [Pt(P-P)₂]₂ is also produced; such ionic species [Pt-(P-P)₂]X₂ are also readily synthesized. Studies on the solubilities of the pyridylphosphine ligands and the Pt and Ru complexes, and their aqueous solution chemistry (including associated p*K*_a values) are in progress.

Ruthenium Complexes. Earlier work from this group^{21a,28} and elsewhere^{21b} has shown that the five-coordinate RuCl₂-(P-P)(PPh₃) species (P-P = dppb, binap, diop) can be made by reaction of 1 equiv of the diphosphine with RuCl₂(PPh₃)₃. The corresponding reaction with racemic dppcp in this study gives rise to *trans*-RuCl₂(dppcp)₂ (**10**) rather than RuCl₂(dppcp)-(PPh₃), which is preferred for catalytic studies.^{21a,24,29} This is in accord with the usual finding that the reaction of RuCl₂(PPh₃)₃ with 1 equiv of the shorter carbon backbone diphosphines Ph₂P-(CH₂)_nPPh₂ (*n* = 1–3) gives rise only to species of the type RuCl₂(P-P)₂, while reaction with diphosphines that form a seven-membered chelate (dppb, binap, diop) yields RuCl₂-(P-P)(PPh₃)₂.^{21,28} This has been attributed to the smaller bite angle of the former set of ligands which leaves the Ru center less sterically crowded and more susceptible to attack by a second diphosphine molecule. The presence of only a single C₂ backbone diphosphine ligand in a Ru(II) complex can be enforced by appropriate choice of the Ru(II) precursor. Thus, in the 1:1 reaction of RuCl₂(dppb)(PPh₃) with dppcp, the complex *trans*-RuCl₂(dppb)(dppcp) (**11**) is formed.

In the reaction of RuCl₂(PPh₃)₃ with 1 equiv of d(py)pcp, a two-carbon backbone phosphine which differs from dppcp only in the presence of 2-pyridyl rather than phenyl rings bound to the P atoms, the availability of pyridyl N atoms allows for bonding of just a single d(py)pcp unit, with six-coordination

Chart 3



resulting from bonding via an N atom; this presumably prevents coordination of a second d(py)pcp ligand. The initially isolated complexes **7a**, **7b**, **8**, and **9**, of the type RuX₂(*P,P,N*-d(py)pcp) (X = halogen), all contain one solvated H₂O molecule as evidenced by ¹H NMR spectroscopy and analytical data. This solvate could not be removed by drying the compounds in vacuo at 100 °C, although crystals of **7a** and **7b** were grown containing solvate CH₂Cl₂ or EtOH, respectively. Complex **12** (*cis*-RuCl₂-(dppb)(*P,N*-PPh₂(py))) had been synthesized previously from the *trans*-isomer, itself made from the reaction of RuCl₂(dppb)-(PPh₃) and PPh₂(py).¹¹

The reaction of 1 equiv of d(py)pe with RuCl₂(PPh₃)₃ in C₆H₆ yields a number of products whose structures are not yet known, and investigation into this reaction is currently underway.

Solution ³¹P{¹H} NMR Spectra. Platinum Complexes. The singlet ³¹P chemical shifts for complexes **1–4** fall in the downfield regime, consistent with the reported relative deshielding of P nuclei in five-membered chelate rings.³⁰ The ¹J_{Pt} values are in the range expected for P nuclei in a *cis* disposition³¹ and singlets imply a C₂ symmetry. The two singlets of roughly equal intensity seen for **5** are attributed to the presence of diastereomers containing combinations of the *R,R* or *S,S* ligand.

Ruthenium Complexes. The ³¹P{¹H} NMR data at r.t. for complexes **7–12** are given in Table 1. The *mer* and *fac* labels, used for convenience, refer to the arrangement of the three coordinated P atoms. Representations of the structures are shown in Chart 3.

In CDCl₃, with the exception of **7b**, the complexes containing P atoms in a *fac* arrangement give rise to ABX or AMX patterns, with diagnostically small ²J_{PP} values (~30 Hz) indicative of mutually *cis* P atoms. On the basis of integration, the downfield resonances for **7–9** are attributed to the d(py)pcp ligand and the more upfield one to PPh₃. Complex **7a** displays two smaller ²J_{PP} values and one larger, consistent with two *cis* and one *trans* coupling constant, i.e., with a *mer* arrangement of the P atoms, as found in the solid-state structure (vide infra).

The ³¹P{¹H} NMR spectrum of **7b** in CDCl₃ at r.t. shows an A₂X triplet and doublet pattern with a coupling constant indicative of three mutually *cis* P atoms (Table 1). The data are consistent with the following solution structures (i) 5-coordinate (square pyramid) geometry in which d(py)pcp acts as a 4-electron *P,P* donor, (ii) 6-coordinate geometry in which d(py)pcp again acts as a *P,P* donor and H₂O is bound in the axial site *trans* to PPh₃ (and note that **7b** is isolated as a monohydrate),

(28) MacFarlane, K. S.; Joshi, A. M.; Rettig, S. J.; James, B. R. *Inorg. Chem.* **1996**, *35*, 7304.

(29) MacFarlane, K. S.; Thorburn, I. S.; Cyr, P. W.; Chau, D. E. K.-Y.; Rettig, S. J.; James, B. R. *Inorg. Chim. Acta* **1998**, *270*, 130.

(30) Dixon, K. R. In *Multinuclear NMR*; Mason, J., Ed.; Plenum: New York, 1987; Chapter 13.

(31) Grim, S. O.; Keiter, R. L.; McFarlane, W. *Inorg. Chem.* **1967**, *6*, 1133.

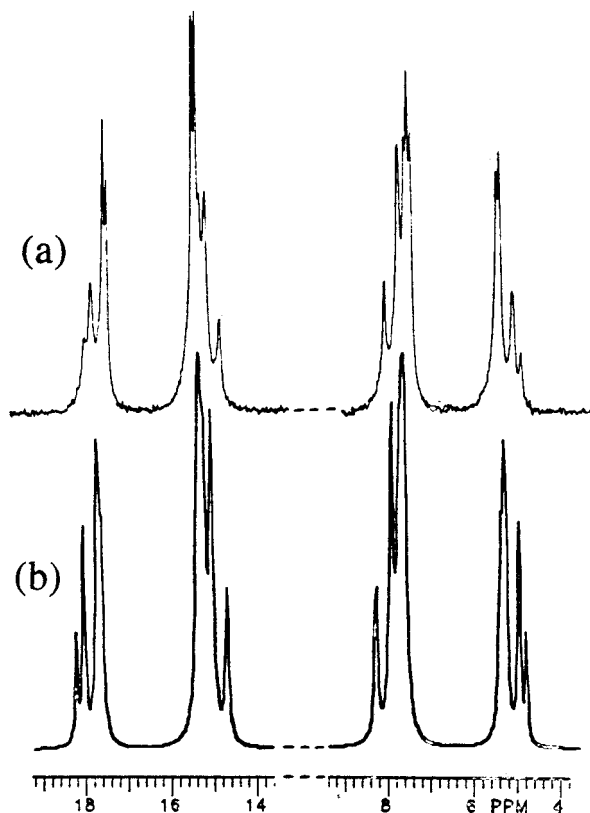


Figure 1. $^{31}\text{P}\{^1\text{H}\}$ NMR spectrum (121.4 MHz, 20 °C) of *trans*- RuCl_2 -(dppb)(dppcp) (**11**) in CDCl_3 ; (a) recorded spectrum and (b) simulated spectrum (AA'BB') obtained using the parameters listed in Table 1.

or (iii) 6-coordinate geometry in which $\text{d}(\text{py})\text{pcp}$ acts as a 6-electron P,P,N donor whose P atoms are rendered equivalent on the NMR time scale by an exchangeable, labile N atom. At -40 °C the spectrum shows the same triplet at 8.8 ppm as observed at r.t., and a 6-line pattern centered at the position of the doublet in the r.t. spectrum (47.8 ppm), which appears to be a superimposition of two triplets (as observed for **7b** at r.t. in C_6D_6 and with the same $^2J_{\text{PP}}$) and the "r.t. doublet". The corresponding -20 °C spectrum is intermediate between those at r.t. and -40 °C; it shows an enhanced "r.t. doublet" overlapped with a diminished pair of triplets centered at 47.8 ppm, as well as the triplet at 8.8 ppm. This rules out possibility (iii) for the r.t. structure which necessitates that at an intermediate temperature, an averaged, broadened signal be observed. Thus, the -20 °C spectrum most probably results from a slow exchange between $\text{RuCl}_2(P,P,N\text{-d}(\text{py})\text{pcp})(\text{PPh}_3)$ and $\text{RuCl}_2(P,P\text{-d}(\text{py})\text{pcp})(\text{PPh}_3)$ (r.t. solution structure (i)) or between $\text{RuCl}_2(P,P,N\text{-d}(\text{py})\text{pcp})(\text{PPh}_3)$ and $\text{RuCl}_2(P,P\text{-d}(\text{py})\text{pcp})(\text{PPh}_3)\text{-}(\text{H}_2\text{O})$ (r.t. structure (ii)).

Of note, the r.t. $^{31}\text{P}\{^1\text{H}\}$ NMR spectrum of **7b** in the less polar solvent C_6D_6 shows an ABX pattern, consistent with the formulation *fac*- $\text{RuCl}_2(P,P,N\text{-d}(\text{py})\text{pcp})(\text{PPh}_3)$ as determined in the solid-state (vide infra).

As with **5**, complex **10** gives rise to two diastereomers as evidenced by the two $^{31}\text{P}\{^1\text{H}\}$ NMR singlets which, in this case, integrate to a ratio of $\sim 2:1$. The greater abundance of one diastereomer over the other is attributed to differences in solubility between the two and not to any kinetic or thermodynamic mechanism of diastereoselectivity.

Complex **11** gives rise to a second-order AA'BB' pattern which is simulated well by the parameters given in Table 1 (Figure 1).

Molecular Structures. Again, for convenience, the solvate

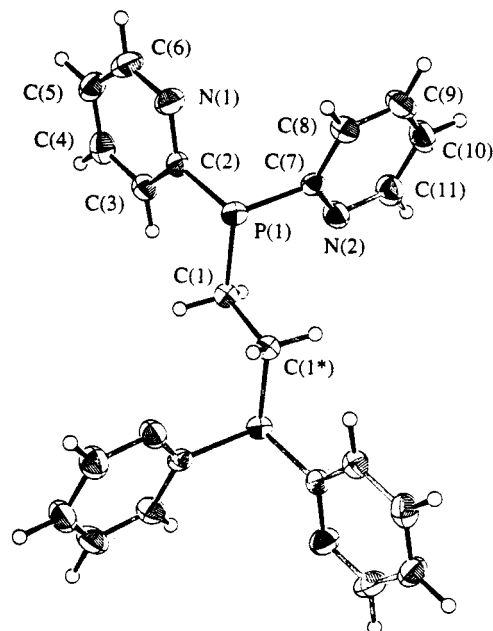


Figure 2. ORTEP representation of $\text{d}(\text{py})\text{pe}$. Thermal ellipsoids for non-hydrogen atoms are drawn at 30% probability.

Table 3. Selected Bond Lengths (Å) and Angles (deg) for $\text{d}(\text{py})\text{pe}$ with Estimated Standard Deviations in Parentheses

P(1)–C(1)	1.842(3)	P(1)–C(2)	1.846(3)
P(1)–C(7)	1.850(3)	N(1)–C(2)	1.346(4)
N(1)–C(6)	1.342(4)	N(2)–C(7)	1.334(4)
N(2)–C(11)	1.338(4)	C(1)–C(1) ^a	1.527(6)
C–C in py rings 1.360(5)–1.384(4)			
C(1)–P(1)–C(2)	101.7(1)	C(1)–P(1)–C(7)	101.8(1)
C(2)–P(1)–C(7)	98.1(1)	C(2)–N(1)–C(6)	116.9(3)
C(7)–N(2)–C(11)	116.6(3)	P(1)–C(1)–C(1) ^a	110.4(3)
P(1)–C(2)–N(1)	112.7(2)	P(1)–C(2)–C(3)	125.4(3)
N(1)–C(2)–C(3)	121.8(3)	N(1)–C(6)–C(5)	124.6(3)
P(1)–C(7)–N(2)	119.9(2)	P(1)–C(7)–C(8)	117.6(3)
N(2)–C(7)–C(8)	122.5(3)	N(2)–C(11)–C(10)	124.6(4)
C–C–C in py rings 117.6(3)–119.9(4)			

^a Symmetry operation: $1 - x, 1 - y, -z$.

molecules associated with the structures are excluded from the number designators of the complexes. The molecular structure of $\text{d}(\text{py})\text{pe}$ shows C_2 symmetry (Figure 2, Table 3). The P–C(CH₂) bond length of 1.842 Å is essentially identical to the average P–C(CH₂) bond length reported for dppe coordinated to various metals (1.845 Å); however, the average P–C(py) bond length (1.848 Å) is significantly longer than the average P–C(Ph) reported for dppe complexes (1.827 Å).³² The average P–C(alkyl and aryl) bond length in free $\text{d}(\text{py})\text{pe}$ is somewhat longer than the corresponding average found for the ligand bound to Pt in **3** (1.846 vs 1.820 Å, respectively). In contrast, the C–C "backbone" distances in the free and coordinated ligands are essentially identical (1.527 and 1.531 Å, respectively). The P(1)–C(1)–C(1*) angles (110°), and the various C–P–C angles (av. 101°) of free $\text{d}(\text{py})\text{pe}$, become 109.5 and 108.5, and 106°, respectively, within **3** (Figure 3). The structure of **3** shows only minor deviations from square-planar geometry at the metal center; the relevant bond angles are shown in Table 4. The $\text{d}(\text{py})\text{pe}$ forms a five-membered chelate ring with Pt(II), through the two P atoms, with the ring atoms (Pt, P(1), C(1), C(2), and P(2)) arranged in a twisted envelope conformation. The average Pt–P bond length (2.210 Å) and

(32) Orpen, A. G.; Brammer, L.; Allen, F. H.; Kennard, O.; Watson, D. G.; Taylor, R. *J. Chem. Soc., Dalton Trans.* **1989**, S1.

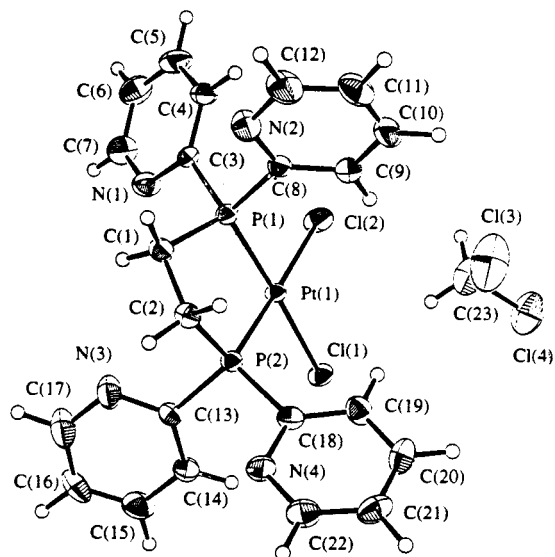


Figure 3. ORTEP representation of *cis*-PtCl₂(d(py)pe)·CH₂Cl₂ (**3**·CH₂Cl₂). Thermal ellipsoids for non-hydrogen atoms are drawn at 33% probability.

Table 4. Selected Bond Lengths (Å) and Angles (deg) for **3**·CH₂Cl₂ with Estimated Standard Deviations in Parentheses

Pt(1)–Cl(1)	2.359(2)	Pt(1)–Cl(2)	2.348(2)
Pt(1)–P(1)	2.209(2)	Pt(1)–P(2)	2.211(2)
P–C 1.810(6)–1.832(6)			
Cl(1)–Pt(1)–Cl(2)	90.80(6)	Cl(1)–Pt(1)–P(1)	177.19(6)
Cl(1)–Pt(1)–P(2)	91.87(6)	Cl(2)–Pt(1)–P(1)	91.18(6)
Cl(2)–Pt(1)–P(2)	177.25(6)	P(1)–Pt(1)–P(2)	86.17(6)
Pt(1)–P(1)–C(1)	108.6(2)	Pt(1)–P(1)–C(3)	113.7(2)
Pt(1)–P(1)–C(8)	115.4(2)	C(1)–P(1)–C(3)	106.9(3)
C(1)–P(1)–C(8)	105.3(3)	C(3)–P(1)–C(8)	106.4(3)
C(2)–C(1)–P(1)	108.5(4)	C(1)–C(2)–P(2)	109.5(4)
C(2)–P(2)–C(13)	105.1(3)	C(2)–P(2)–C(18)	105.7(3)
Pt(1)–P(2)–C(2)	109.5(2)	Pt(1)–P(2)–C(13)	115.5(2)
Pt(1)–P(2)–C(18)	115.6(2)	C(2)–P(2)–C(13)	105.1(3)
C(2)–P(2)–C(18)	105.7(3)	C(13)–P(2)–C(18)	104.5(3)
P(1)–C(8)–N(2)	114.1(5)	P(1)–C(3)–N(1)	112.3(5)
P(2)–C(18)–N(4)	114.0(5)	P(2)–C(13)–N(3)	114.3(5)

P–Pt–P angle (86.17°) are essentially identical with those determined for *cis*-PtCl₂(dpe) (2.208 Å and 86.3°).³³

The structure of **2** shows only slight deviations from square-planar geometry at the metal center (Figure 4); the bond angles and lengths for both crystallographically independent molecules are shown in Table 5. The d(py)pcp forms a five-membered chelate ring again with bonding via the two P atoms. The chirality at the methine carbon atoms in the d(py)pcp ligand backbone shown in Figure 4 is *S,S*, and the chelate ring is in the δ configuration; the same is true for the second crystallographically independent molecule. The *R,R* enantiomers must also be present in the unit cell, as racemic d(py)pcp was used in the preparation of **2** which crystallized in the nonchiral space group *P2₁/c*. The average Pt–P bond length (2.246 Å) is somewhat longer than that observed in **3** (2.210 Å), perhaps due to the stronger trans influence of iodide versus chloride, although the comparison is drawn between two nonidentical P–P ligand systems.

The structure of **7a** (Figure 5, Table 6) is distorted from octahedral coordination because of the four-membered P–N chelate ring; for example, the N(1)–Ru(1)–P(2) bond angle is a constrained 69.43°, while the P(2)–Ru(1)–Cl(1) bond angle

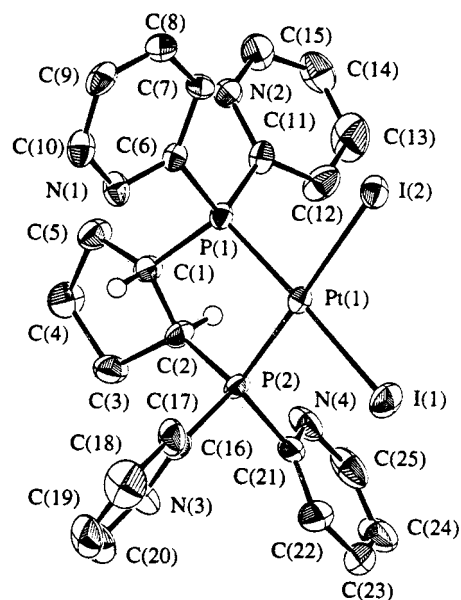


Figure 4. ORTEP representation of one of the two crystallographically independent molecules of *cis*-PtI₂(d(py)pcp) (**2**) in the asymmetric unit (50% probability ellipsoids).

Table 5. Selected Bond Lengths (Å) and Angles (deg) for **2**·0.18 CH₂Cl₂ with Estimated Standard Deviations in Parentheses

Pt(1)–I(1)	2.639(1)	Pt(1)–I(2)	2.653(1)
Pt(1)–P(1)	2.244(2)	Pt(1)–P(2)	2.247(2)
Pt(2)–I(3)	2.651(1)	Pt(2)–I(4)	2.653(1)
Pt(2)–P(3)	2.243(2)	Pt(2)–P(4)	2.248(2)
C(1)–C(2)	1.480(1)	C(26)–C(27)	1.547(1)
P–C 1.808(8)–1.839(8)			
I(1)–Pt(1)–I(2)	91.43(2)	I(1)–Pt(1)–P(1)	176.18(5)
I(1)–Pt(1)–P(2)	92.08(5)	I(2)–Pt(1)–P(1)	88.98(5)
I(2)–Pt(1)–P(2)	175.07(5)	P(1)–Pt(1)–P(2)	87.75(7)
I(3)–Pt(2)–I(4)	92.38(2)	I(3)–Pt(2)–P(3)	178.01(5)
I(3)–Pt(2)–P(4)	91.17(5)	I(4)–Pt(2)–P(3)	89.38(5)
I(4)–Pt(2)–P(4)	176.15(5)	P(3)–Pt(2)–P(4)	87.05(7)
P(1)–C(6)–N(1)	113.4(6)	P(1)–C(11)–N(2)	117.6(5)
P(2)–C(16)–N(3)	115.0(6)	P(2)–C(21)–N(4)	113.9(6)
P(3)–C(31)–N(5)	117.1(6)	P(3)–C(36)–N(6)	111.0(6)
P(4)–C(41)–N(7)	112.2(5)	P(4)–C(46)–N(8)	116.2(5)

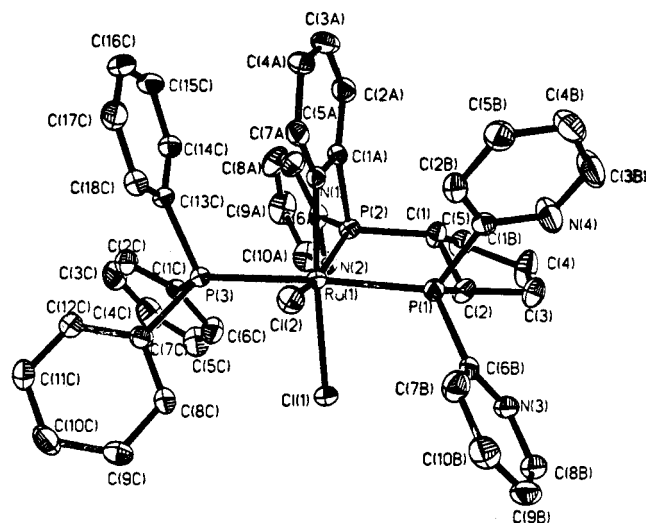


Figure 5. ORTEP representation of *mer*-RuCl₂(P,P,N,N-d(py)pcp)(PPh₃) (**7a**) (50% probability ellipsoids).

is relaxed to 104.70°, i.e., the P(2) atom is bent toward the N(1) atom. The P–C–N(coordinated) angles for the four-membered rings in **7a**, **7b**, and **12** are similar (100.5, 100.8, and 103.0°,

(33) Farrar, D. H.; Ferguson, G. J. *Crystallogr. Spectrosc. Res.* **1982**, *12*, 465.

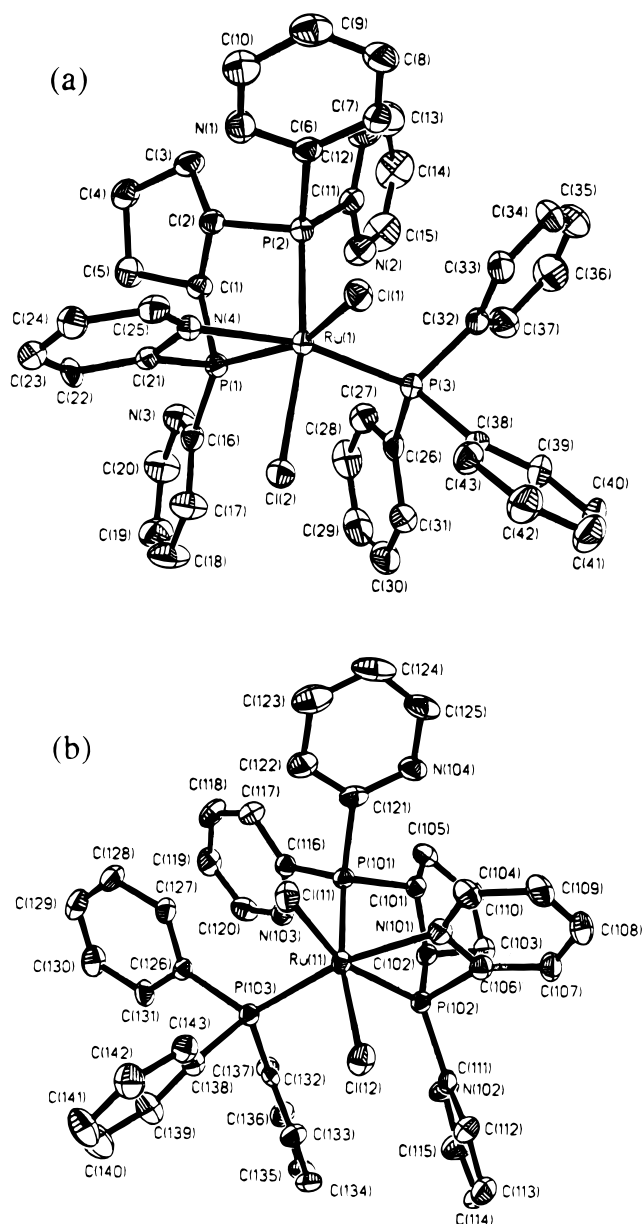
Table 6. Selected Bond Lengths (Å) and Angles (deg) for **7a**·2CH₂Cl₂ with Estimated Standard Deviations in Parentheses

Ru(1)–N(1)	2.078(3)	Ru(1)–P(2)	2.269(1)
Ru(1)–P(1)	2.364(1)	Ru(1)–P(3)	2.394(1)
Ru(1)–Cl(2)	2.443(1)	Ru(1)–Cl(1)	2.452(1)
N–C 1.336(5)–1.364(5)			
P–C 1.830(4)–1.858(4)			
N(1)–Ru(1)–P(2)	69.43(9)	N(1)–Ru(1)–P(1)	93.77(9)
P(2)–Ru(1)–P(1)	82.26(4)	N(1)–Ru(1)–P(3)	89.85(9)
P(2)–Ru(1)–P(3)	99.29(4)	P(1)–Ru(1)–P(3)	176.37(4)
N(1)–Ru(1)–Cl(2)	90.55(9)	P(2)–Ru(1)–Cl(2)	158.44(4)
P(1)–Ru(1)–Cl(1)	91.49(4)	P(3)–Ru(1)–Cl(2)	88.21(4)
N(1)–Ru(1)–Cl(1)	173.62(9)	P(2)–Ru(1)–Cl(1)	104.70(4)
P(1)–Ru(1)–Cl(1)	82.76(4)	P(3)–Ru(1)–Cl(1)	93.66(4)
P(1)–C(6B)–N(3)	116.3(3)	P(1)–C(1B)–N(4)	115.8(3)
P(2)–C(6A)–N(2)	112.7(3)	P(2)–C(1A)–N(1)	100.5(3)

respectively) and are severely compressed when compared to the values for the average P–C–N(free) angles of 114.6, 113.7, 116.3, 115.0, and 114.4° found in **2**, **3**, d(py)pe, **7a**, and **7b**, respectively. Complex **7a** displays a mer arrangement of the three P atoms, and a cis disposition of the two Cl atoms, with the coordinated pyridyl N atom trans to a Cl atom. The coordinated P(1) atom of the d(py)pcp ligand bearing the two noncoordinated pyridyl groups is trans to PPh₃ and shows a significantly longer Ru–P bond than the P(2) atom which is trans to the lower trans influence Cl atom (2.3636 vs 2.2687 Å). The five-membered P–P chelate of d(py)pcp is in the λ configuration.

On coordination of the N atom of the pyridyl group, the associated P atom of d(py)pcp becomes chiral, and the ORTEP (Figure 5) shows the *S* configuration. Furthermore, in the preparation of **7a**, a racemic (*R,R* and *S,S*) mixture of d(py)pcp was used, while the ORTEP shows the *R,R* configuration. The mirror image of the structure given in Figure 5, i.e., the *R,S,S* enantiomer, is not shown, but the isolated crystal, belonging again to the symmetric space group *P*, must contain one molecule of each enantiomeric form in the unit cell. The *R,R,R* and the *S,S,S* isomers were not crystallographically observed, nor does the solution ³¹P{¹H} NMR spectrum indicate the presence of diastereomers.

The ORTEP of complex **7b** (Figures 6a and b, Table 7) evidences a distorted octahedral arrangement around the Ru atom, again imposed by constraints of the four-membered P–N chelate of the d(py)pcp ligand; the N(4)–Ru(1)–P(1) bond angle is only 67.85° while the P(1)–Ru(1)–P(3) bond angle is 106.94°. Complexes **7a** and **7b** are structural isomers: both display *cis*-chloro ligands, but in **7b** the three P atoms are arranged in a *fac* as opposed to the *mer* fashion seen in **7a**, and the ligand trans to the coordinated pyridyl N atom is PPh₃ (vs the Cl atom for **7a**). The Ru–P bond lengths for the coordinated d(py)pcp in **7b**, with both P atoms being trans to Cl, are essentially identical (2.2873 and 2.2863 Å). In addition, the Ru–PPh₃ bond length in **7b** (2.3056 Å) is shorter than in **7a** (2.3941 Å) because of the weaker trans influence of N with respect to P. The solid-state structure of **7b** is consistent with the ³¹P{¹H} NMR spectrum measured in C₆D₆ (see above). The unit cell of **7b**·1.5EtOH contains two crystallographically independent molecules of **7b** which have marginally different geometrical parameters (Table 7), and belongs to the centrosymmetric space group *P* with a *Z* value of 4. This necessitates the presence of both enantiomeric forms of each of the crystallographically independent molecules within the unit cell. The ORTEP representations in Figure 6a and b correspond to the *S,S,S* enantiomer of one independent molecule and the *R,R,R* enantiomer of the other, respectively. In this instance, the *R,S,S*

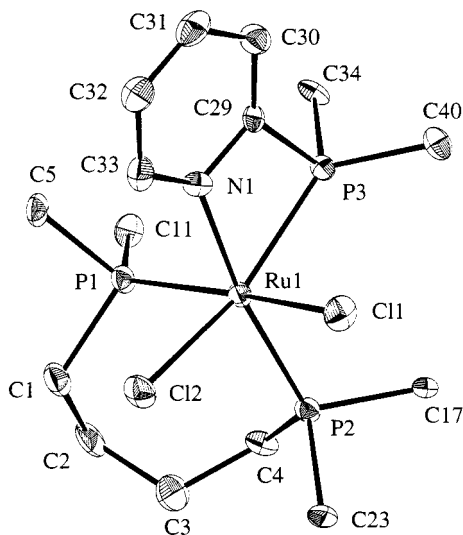
**Figure 6.** ORTEP representations of the two crystallographically independent molecules of *fac*-RuCl₂(*P,P,N*-d(py)pcp)(PPh₃) (**7b**) in the asymmetric unit (50% probability ellipsoids); (a) and (b) show the *S,S,S* and *R,R,R* diastereomers, respectively.

and *S,R,R* isomers were not crystallographically observed. In **2**, **7a**, and both crystallographically independent forms of **7b**, an *R,R* configuration of the ligand backbone enforces a λ conformation in the five-membered P–P chelate ring, while the *S,S* configuration enforces a δ conformation. However, the absolute configuration at the P atom bearing the coordinated pyridyl group has no effect upon the envelope conformation.

The distortion from octahedral geometry enforced by a four-membered chelate is evidenced once more in the structure of **12** (Figure 7, Table 8). The P–N chelate ring of PPh₂(py) displays a N(1)–Ru(1)–P(3) angle of 68.0° and a P(1)–Ru(1)–P(3) angle of 101.1°, similar to the values found for the corresponding angles in **7a** and **7b**. Although the ligand set in **12** is different, the three P atoms (two from dppb and one from PPh₂(py)) are also in a *fac* arrangement. The structure reported here for **12** is consistent with the previously reported solution structure, based on a ³¹P{¹H} AMX pattern; the designators A and M refer to the dppb P atoms, and X designates the PPh₂-

Table 7. Selected Bond Lengths (Å) and Angles (deg) for **7b**·1.5EtOH with Estimated Standard Deviations in Parentheses

Ru(1)–N(4)	2.141(4)	Ru(1)–P(1)	2.286(1)
Ru(1)–P(2)	2.287(1)	Ru(1)–P(3)	2.306(1)
Ru(1)–Cl(1)	2.455(1)	Ru(1)–Cl(2)	2.481(1)
P–C 1.825(5)–1.857(6)			
N(4)–Ru(1)–P(1)	67.85(11)	N(4)–Ru(1)–P(2)	91.13(11)
P(1)–Ru(1)–P(2)	83.94(5)	N(4)–Ru(1)–P(3)	166.85(11)
P(1)–Ru(1)–P(3)	106.94(5)	P(2)–Ru(1)–P(3)	100.45(5)
N(4)–Ru(1)–Cl(1)	89.64(11)	P(1)–Ru(1)–Cl(1)	157.04(5)
P(2)–Ru(1)–Cl(1)	92.33(5)	P(3)–Ru(1)–Cl(1)	96.02(5)
N(4)–Ru(1)–Cl(2)	80.76(11)	P(1)–Ru(1)–Cl(2)	88.62(5)
P(2)–Ru(1)–Cl(2)	170.63(5)	P(3)–Ru(1)–Cl(2)	87.15(5)
Cl(1)–Ru(1)–Cl(2)	92.31(5)	P(1)–C(21)–N(4)	100.8(3)
P(1)–C(16)–N(3)	115.5(4)	P(2)–C(11)–N(2)	113.9(4)
P(2)–C(6)–N(1)	114.8(4)		
Ru(11)–N(101)	2.138(4)	Ru(11)–P(102)	2.271(1)
Ru(11)–P(101)	2.291(1)	Ru(11)–P(103)	2.313(1)
Ru(11)–Cl(11)	2.459(1)	Ru(11)–Cl(12)	2.470(1)
P–C 1.825(5)–1.846(5)			
N(101)–Ru(11)–P(101)	87.80(12)	P(102)–Ru(11)–P(101)	84.40(5)
N(101)–Ru(11)–P(103)	168.30(11)	P(102)–Ru(11)–P(103)	102.71(5)
P(101)–Ru(11)–P(103)	99.49(5)	N(101)–Ru(11)–P(102)	68.71(11)
N(101)–Ru(11)–Cl(11)	89.36(11)	P(102)–Ru(11)–Cl(11)	158.06(5)
P(101)–Ru(11)–Cl(11)	94.66(5)	P(103)–Ru(11)–Cl(11)	99.07(5)
N(101)–Ru(11)–Cl(12)	82.92(11)	P(102)–Ru(11)–Cl(12)	88.84(5)
P(101)–Ru(11)–Cl(12)	170.04(5)	P(103)–Ru(11)–Cl(12)	89.11(5)
Cl(11)–Ru(11)–Cl(12)	88.88(5)	P(102)–C(106)–N(101)	100.9(3)
P(102)–C(111)–N(102)	113.6(4)	P(101)–C(116)–N(103)	111.5(3)
P(101)–C(121)–N(104)	116.8(4)		

**Figure 7.** ORTEP representation of *cis*-RuCl₂(dppb)(*P,N*-PPh₂(py)) (**12**). Thermal ellipsoids for non-hydrogen atoms are drawn at 50% probability. Some of the phenyl carbon atoms have been omitted for clarity.

(py) P atom. The structure is comparable to those of *cis*-RuCl₂-(dppb)(*N,N*) (*N,N* = 2,2'-bipyridine or *o*-phenanthroline) that contain the "less compressed" five-membered chelate rings with *N*–Ru–*N* angles of 76.7 and 78.2°, respectively.³⁴

Preliminary Catalysis Results. Preliminary results show that the complexes *fac*-RuX₂(*P,P,N-d*(py)pcp)(PPh₃) (X = Cl, Br, I; **7b**, **8**, and **9**, respectively) can effect the homogeneous catalytic hydrogenation of imines to amines. The experiments were performed under conditions employed previously in this laboratory to allow for comparison with data obtained with "Ru^{II}-(*P-P*)" catalytic precursors (using 1000 psi of H₂, at r.t. in

Table 8. Selected Bond Lengths (Å) and Angles (deg) for **12** with Estimated Standard Deviations in Parentheses

Ru(1)–Cl(1)	2.460(1)	Ru(1)–Cl(2)	2.430(1)
Ru(1)–P(1)	2.314(1)	Ru(1)–P(2)	2.316(1)
Ru(1)–P(3)	2.348(1)	Ru(1)–N(1)	2.146(3)
P–C 1.826(4)–1.854(5)			
Cl(1)–Ru(1)–Cl(2)	85.65(4)	Cl(1)–Ru(1)–P(1)	168.18(4)
Cl(1)–Ru(1)–P(2)	91.36(4)	Cl(1)–Ru(1)–P(3)	85.84(5)
Cl(1)–Ru(1)–N(1)	81.2(1)	Cl(2)–Ru(1)–P(1)	84.48(5)
Cl(2)–Ru(1)–P(2)	93.41(4)	Cl(2)–Ru(1)–P(3)	158.30(4)
Cl(2)–Ru(1)–N(1)	90.9(1)	P(1)–Ru(1)–P(2)	95.71(5)
P(1)–Ru(1)–P(3)	101.11(5)	P(1)–Ru(1)–N(1)	92.4(1)
P(2)–Ru(1)–P(3)	106.71(4)	P(2)–Ru(1)–N(1)	171.1(1)
P(3)–Ru(1)–N(1)	68.0(1)	Ru(1)–P(1)–C(1)	117.5(2)
Ru(1)–P(1)–C(5)	107.9(2)	Ru(1)–P(1)–C(11)	125.9(2)
C(1)–P(1)–C(5)	101.1(2)	C(1)–P(1)–C(11)	99.2(2)
C(5)–P(1)–C(11)	101.7(2)	Ru(1)–P(2)–C(4)	118.4(1)
Ru(1)–P(2)–C(17)	113.5(2)	Ru(1)–P(2)–C(23)	119.4(1)
C(4)–P(2)–C(17)	101.2(2)	C(4)–P(2)–C(23)	102.0(2)
C(17)–P(2)–C(23)	99.2(2)	Ru(1)–P(3)–C(29)	83.6(2)
Ru(1)–P(3)–C(34)	129.4(2)	Ru(1)–P(3)–C(40)	128.2(2)
C(29)–P(3)–C(34)	105.1(2)	C(29)–P(3)–C(40)	105.6(2)
C(34)–P(3)–C(40)	97.9(2)	P(3)–C(29)–N(1)	103.0(3)

MeOH (10 mL) with 0.77 mM Ru complex and 0.153 M imine substrate).^{24,29} The conversions of PhC(H)=NPh to PhCH₂N-(H)Ph under these conditions after 3 h were 80, 99, and 63% for the chloro, bromo, and iodo complexes, respectively. For comparison, under the same conditions, the dinuclear species [RuX(dppb)]₂(μ-X)₂ catalyzed the hydrogenation of PhC(H)=NPh with conversions of 24 (X = Cl), 74 (X = Br), and 100% (X = I).²⁹ The hydrogenation of a second imine substrate PhC(H)=NCH₂Ph was also investigated using **7b**, **8**, and **9** as precursor catalysts. Under the same conditions outlined above, but for 1 h reaction time, the conversions to dibenzylamine were 5 (X = Cl), 10 (X = Br), and 28% (X = I) while [RuCl(dppb)]₂-(μ-Cl)₂ was much more active, giving 87% conversion.²⁹

Although the catalytic results are preliminary, they illustrate again the important role that the halogen plays in imine

(34) Quieroz, S. J.; Batista, A. A.; Oliva, G.; do P. Gambardella, M. T.; Santos, R. H. A.; MacFarlane, K. S.; Rettig, S. J.; James, B. R. *Inorg. Chim. Acta* **1998**, 267, 209.

hydrogenations,^{29,35} and that the comparison of reactivity between complexes may be substrate dependent. The RuCl₂-(d(py)pcp)(PPh₃) complex in the solid state and in benzene contains a *P*₃*N* donor ligand set, while in CDCl₃ there is NMR evidence for some lability of the N atom; whether such behavior is involved in the catalysis in MeOH is as yet unknown, but the catalytic activity is good, and further studies, particularly at making hydrido derivatives, are at hand. The facile syntheses and air-stability of the RuX₂(d(py)pcp)(PPh₃) complexes make them attractive as catalyst precursors. Resolution of the chiral d(py)pcp would allow investigation into catalytic asymmetric hydrogenation. Of note, Noyori's group has used a tetradentate, diphosphine/diamine *P*₂*N*₂ donor set (which contains chirality at methine C atoms of a cyclohexane ring that bridges the N atoms) within a *trans*-RuCl₂(P₂N₂) complex that catalyzes effective transfer hydrogenations of imines (from 2-propanol).³⁶

Conclusions

A new 2-pyridyldiphosphine ligand, d(py)pcp, has been synthesized as a racemate and its coordination at Pt(II) and Ru(II) centers investigated. The *P,P*- and *P,P,N*-bonding modes are found at the Pt(II) and Ru(II) centers, respectively, the latter

incorporating a *P,N*-chelate ring, where there is also some evidence for lability of the N atom. The Ru-d(py)pcp complexes are effective precursors for catalytic H₂ hydrogenation of aldimines in MeOH solution. The related ligand d(py)pe, the 2-pyridyl analogue of the well-known diphos, has been shown to exhibit *P,P* bonding at Pt(II). Of special interest, but not described here, d(py)pe and several of the complexes have some solubility in water, and are freely soluble in dilute aqueous acid solution. The aqueous solution chemistry of these pyridyl-diphosphine systems, and their potential for homogeneous catalysis in aqueous media, are currently being studied.

Acknowledgment. We thank the Natural Sciences and Engineering Research Council of Canada for financial support, Johnson Matthey Ltd. and Colonial Metals Inc. for the loans of RuCl₃·*x*H₂O and K₂[PtCl₄], the Royal Society for the award of a fellowship to M.B.S., and Dr. V. G. Young, Jr. (X-ray Crystallographic Laboratory, University of Minneapolis) for determination of the structures of **7a** and **7b**.

Supporting Information Available: Tables of atomic coordinates and equivalent isotropic thermal parameters, hydrogen atom parameters, anisotropic thermal parameters, complete lists of bond lengths and angles, and torsion angles for the structures of d(py)pe, **2**, **3**, **7a**, **7b**, and **12**. This material is available free of charge via the Internet at <http://pubs.acs.org>.

IC990002O

(35) James, B. R. *Catal. Today* **1997**, *37*, 209.

(36) Noyori, R.; Hashiguchi, S. *Acc. Chem. Res.* **1997**, *30*, 97.